Morphology and Thermal Stability of the Active Layer in Poly(*p*-phenylenevinylene)/Methanofullerene Plastic Photovoltaic Devices

Xiaoniu Yang,[†,⊥] Jeroen K. J. van Duren,[‡] René A. J. Janssen,[‡,⊥] Matthias A. J. Michels,[†,⊥] and Joachim Loos*[,§,⊥]

Group Polymer Physics, Molecular Materials and Nanosystems, and Laboratories of Polymer Technology and Solid State Chemistry and Materials, Eindhoven University of Technology, PO Box 513, NL-5600 MB Eindhoven, The Netherlands, and Dutch Polymer Institute, PO Box 902, NL-5600 AX Eindhoven, The Netherlands

Received October 28, 2003; Revised Manuscript Received January 8, 2004

ABSTRACT: The morphology of composite thin films consisting of a conjugated polymer (poly[2-methoxy-5-(3′,7′-dimethyloctyloxy)-1,4-phenylenevinylene], MDMO-PPV) and methanofullerene ([6,6]-phenyl C_{61} butyric acid methyl ester, PCBM), which are used as the active layer in polymer photovoltaic devices, has been extensively studied using transmission electron microscopy (TEM) and selected-area electron diffraction (SAED). Composite MDMO-PPV:PCBM films have been prepared with PCBM concentrations varying from 20 to 90 wt %. PCBM-rich clusters are clearly observed in TEM bright-field mode when the PCBM concentration is increased to ca. 75 wt % in the composite film. The SAED analysis shows that these clusters consist of many PCBM nanocrystals with random crystallographic orientations. Furthermore, we show that these nanocrystals are also present in the homogeneous matrix at PCBM concentrations below 75 wt %. Annealing of the blend films has been performed at temperatures between 60 and 130 °C for different times. In all cases, but especially when the annealing temperature is above the glass transition temperature of MDMO-PPV (∼80 °C), PCBM molecules show high diffusion mobility, resulting in accelerated phase segregation and in the formation of large PCBM single crystals in the film. The observed phase segregation, even at temperatures as low as 60 °C, indicates that the thermal stability of MDMO-PPV:PCBM films will likely limit the long-term performance of solar cells based on these materials.

Introduction

A bicontinuous interpenetrating network structure between electron donor and acceptor materials, or bulk heterojunction, is one of the most promising morphological architectures for the active layer in photovoltaic cells and has provided energy conversion efficiencies as high as $\eta = 2.5-3.5\%$ in simulated solar light.[1−10] In contrast to many inorganic semiconductors, in which photon absorption directly produces free electrons and holes,[11] optical absorption in organic molecular and polymer semiconductors mainly creates electron−hole pairs (excitons) that are bound at room temperature.[12] In bulk heterojunction photovoltaic cells the creation of free electrons and holes is accomplished by the spontaneous dissociation of the excitons at the donor/acceptor interface. Subsequent transport and collection of the photoinduced charges at the appropriate electrodes then provides the photovoltaic effect.

For active layers consisting of blends of functional polymers (or low molecular weight organic molecules), it is essential to control the morphology and create interpenetrating networks with nanoscale phase separation between electron donor and acceptor materials to achieve the optimum performance.[1−10,13−19] It has been established that both the conditions for solution processing[5,9,15,16] and thermal treatment of as-prepared films[7,10,17−19] can strongly influence the performance of these devices because they affect the morphology of the bulk heterojunction. The reason for that is twofold. First of all, the dimension of the phase separation determines the average distance that excitons have to diffuse to reach the donor−acceptor interface where they can be dissociated. Because the exciton diffusion range in the polymer is typically limited to around 10 nm,[20−22] the amount of photogenerated charges is related to the scale of phase separation. Second, interpenetrating networks ensure continuous pathways for both charges to reach the appropriate electrodes and are a prerequisite for effective charge collection.

For future application of polymer photovoltaic devices, both their efficiency and lifetime must be improved. In this respect the morphology of the active layer and its long-term and thermal stability are of interest. For the MDMO-PPV:PCBM blend system, a rapid decrease in performance of sealed devices has already been observed even after thermal aging at around 45−50 °C in the dark.[23] The most widely used technique to deposit active layers for polymer photovoltaic devices is spin-coating. In this technique the solvent rapidly evaporates, and together with confinement the rapid drying results in thin films that are far away from their equilibrium morphological state, particularly for long chain polymers.[24,25] From a viewpoint of thermodynamics, such a kinetically determined morphology is prone to further relaxation and reorganization on a molecular and mesoscopic scale. This reorganization will always occur with

* To whom correspondence should be addressed. Email: j.loos@tue.nl. Phone: (31) 40-2473033.
† Group Polymer Physics, Eindhoven University of Technology.
‡ Molecular Materials and Nanosystems, Eindhoven University of Technology.
§ Laboratories of Polymer Technology and Solid State Chemistry and Materials, Eindhoven University of Technology.
⊥ Dutch Polymer Institute.

10.1021/ma035620+ CCC: $27.50
Published on Web 02/21/2004

time, although maybe not on a short time scale; however, it is accelerated at elevated temperatures.

Here we present a study on the morphology and thermal stability of a blend of a conjugated polymer (poly[2-methoxy-5-(3′,7′-dimethyloctyloxy)-1,4-phenylenevinylene], MDMO-PPV)[26] and a methanofullerene derivative ([6,6]-phenyl C_{61} butyric acid methyl ester, PCBM)[27] that has become one of the most intensely studied material combinations after it has been established to give 2.5% efficient solar cells.[5] In a recent study we have shown that pure PCBM forms thin films consisting of many randomly oriented nanocrystals when cast from solution under conditions where the solvent evaporates quickly.[28] Merely in view of the size effect,[24,25,29−32] the morphological stability of nanocrystalline PCBM films is limited. Indeed, it has been shown in the same study that pure PCBM films reorganize to form larger crystallites when being annealed. On the basis of this experience, it is the purpose of the present study to investigate the effect of the preparation conditions (such as spin-coating, drop-casting, different solvents, and PCBM concentrations) on the film morphology and to determine the changes in morphology of MDMO-PPV:PCBM composite films upon annealing by using transmission electron microscopy (TEM) and selected-area electron diffraction (SAED).

Experimental Part

Mixed solutions were prepared by dissolving MDMO-PPV (synthesized via the Gilch route)[26] and PCBM[27] in the desired solvent (chlorobenzene or toluene) and continuously stirring in the dark overnight. The concentration of the solution and spin-coating parameters were adjusted to provide homogeneous films with thickness around 100 nm. Unless stated otherwise, spin-coated films were prepared following the same procedures used in device fabrication. Hence, ITO-covered glass substrates were first cleaned by ultrasonic treatment in acetone, followed by rubbing with soap, rinsing in demineralized water, and refluxing with 2-propanol to remove water. Finally, the substrates were treated in a UV-ozone oven for ca. 20 min. Subsequently, poly(ethylenedioxythiophene):poly(styrenesulfonate) (PEDOT:PSS, Bayer AG, Germany) was spin-coated from an aqueous dispersion on the cleaned substrates. This layer was dried by heating on a hot plate at 180 °C for ca. 1 min, followed by cooling on a plate at 25 °C during 1 min. In the final step, the active layer was spin-coated on top of the PEDOT:PSS layer from a solution containing MDMO-PPV:PCBM.

To prepare specimens for TEM investigation, the spin-coated MDMO-PPV:PCBM films were floated onto the surface of deionized water and finally picked up by a 400 mesh copper grid. For drop-cast films, TEM specimens were obtained by putting a droplet of the MDMO-PPV:PCBM solution onto a carbon film supported copper grid. The solvent was evaporated in ambient environment in the dark.

Annealing of samples was performed under precisely controlled temperature and atmosphere conditions, using a Linkam apparatus (model TMS94) equipped with THMS600 temperature stage. During the whole annealing process, the sample was kept in a dark chamber with continuous flow of dry argon to prevent oxidization induced by light, oxygen, water, and/or the high temperature. The stability of the temperature was controlled within 0.1 °C. The annealing experiments were started by rapidly heating (130 °C/min) the samples from room temperature (between 20 and 25 °C) to the desired annealing temperatures. After annealing the samples were cooled to room temperature at the same rate (130 °C/min).

Bright-field TEM morphology observations and acquisition of SAED patterns were conducted on a JEOL JEM-2000FX transmission electron microscope operated at 80 kV. In both cases for bright-field imaging and SAED recording the exposure time was chosen that neither morphological changes could be monitored (for BF) nor the crystalline structure of the samples was destroyed (for SAED). In general, the stability of PCBM crystals under electron beam illumination is much better compared to most polymer samples. Traditional negative plates were used to record all the images. Then, the negatives were digitized using a high-resolution scanner (Agfa DUO scanner) working in gray mode with 8 bits/channel of gray scale. The physical scanning resolution of the negatives was usually between 800 and 1200 dpi.

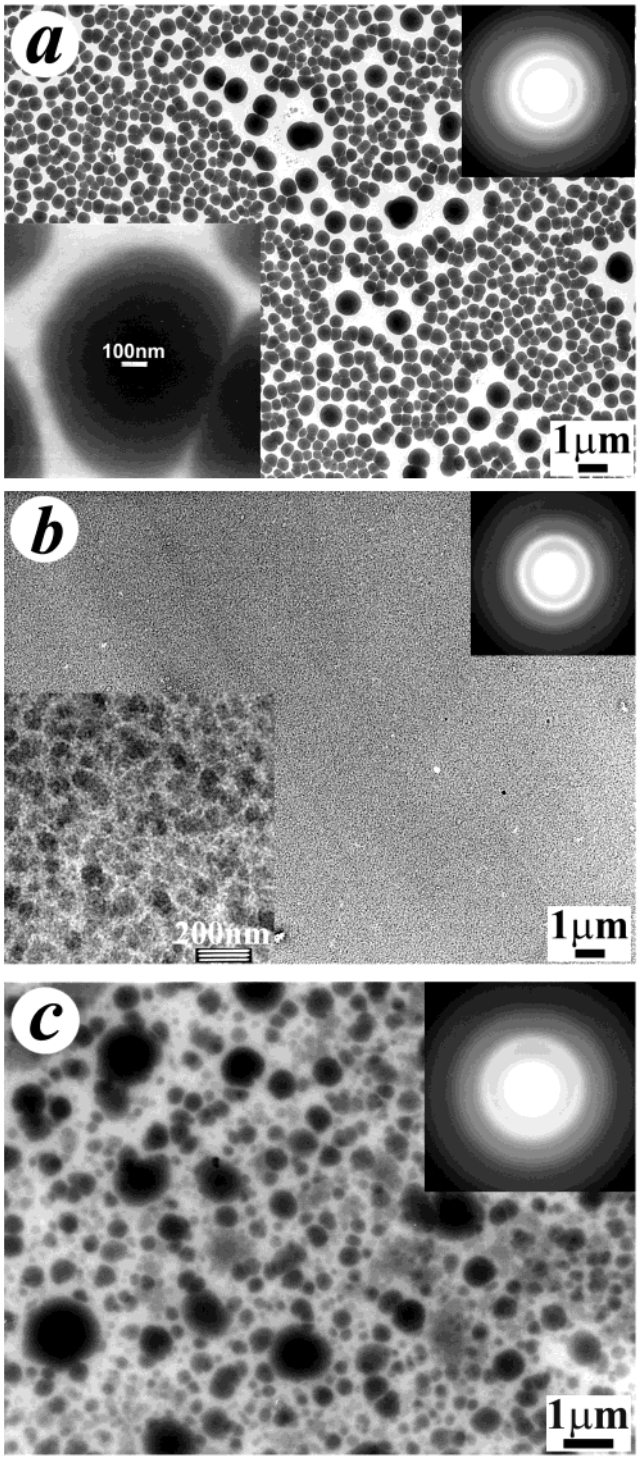

Figure 1. Bright-field TEM images of MDMO-PPV:PCBM films (1:4 wt ratio) prepared by spin-coating from toluene (a) and chlorobenzene (b) and by drop-casting from chlorobenzene (c). The insets represent the corresponding SAED patterns.

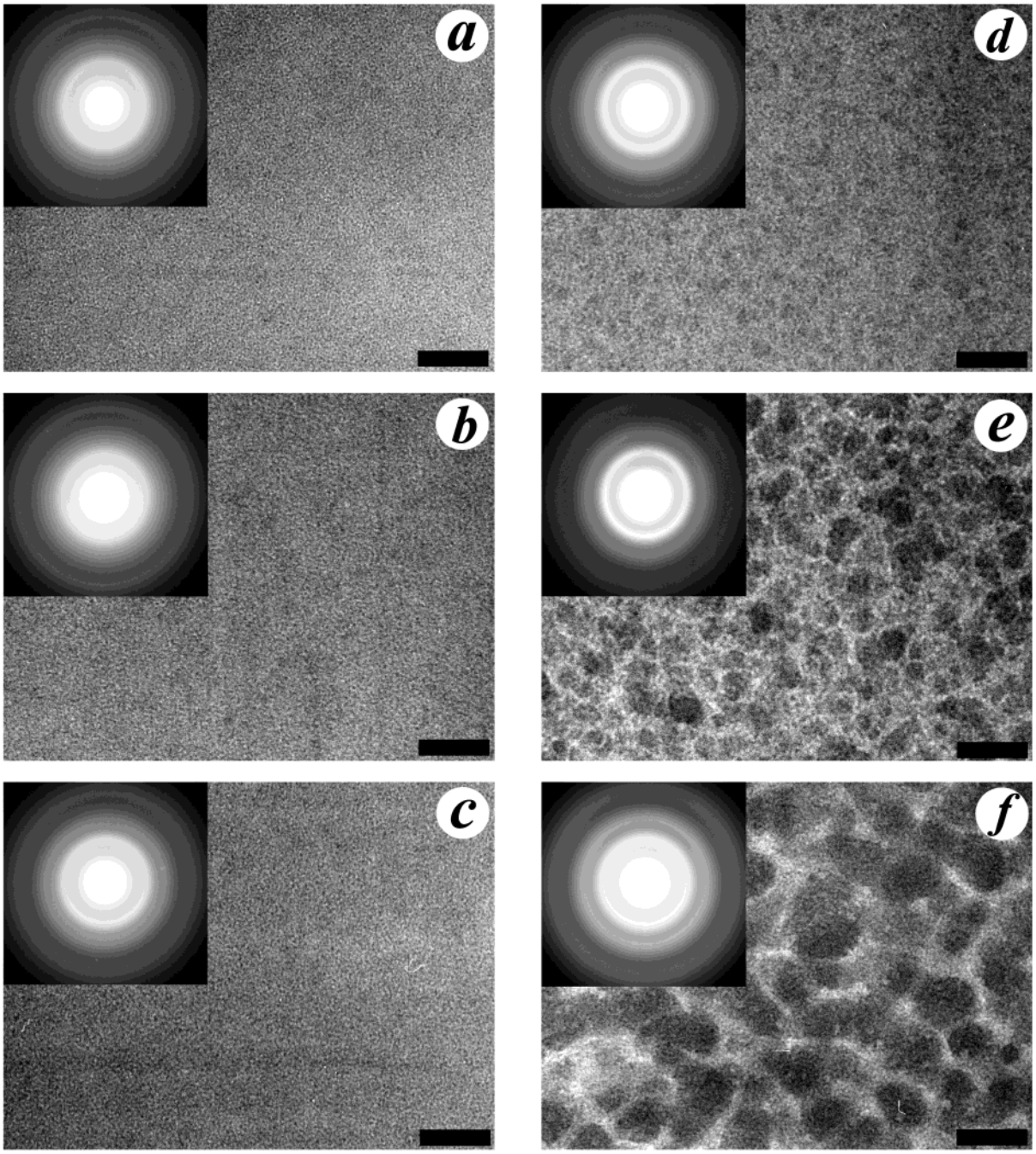

Figure 2. Bright-field TEM images (scale bar: 200 nm) and corresponding SAED patterns of MDMO-PPV:PCBM films prepared via spin-coating from chlorobenzene with PCBM concentrations of (a) 20, (b) 40, (c) 60, (d) 75, (e) 80, and (f) 90 wt %.

Results and Discussion

Influence of the Solvent and Evaporation Rate on the Film Morphology. Bright-field TEM images clearly reveal that phase segregation occurs in composite MDMO-PPV:PCBM (1:4 weight ratio) films, spin-coated from toluene (Figure 1a) and chlorobenzene (Figure 1b). In the TEM images, the dark areas are attributed to PCBM-rich domains because the electron scattering density of PCBM is much higher than that of MDMO-PPV,[33] and the thickness is rather homogeneous (rms roughness of ~4 nm, as verified by atomic force microscopy) for the film prepared from chlorobenzene. The TEM images demonstrate a morphology in which PCBM-rich domains are dispersed in an MDMO-PPV-rich matrix.[13] The size of the PCBM-rich domains in the blend films, however, changes tremendously with the choice of solvent.[5,13] Using toluene (Figure 1a), the average size of the PCBM-rich domains is around 600 nm with a broad size distribution (roughly 350−1300 nm). In contrast, the size of PCBM clusters is quite small with about 80 nm when prepared from chlorobenzene solution. The solubility of both MDMO-PPV and PCBM in toluene is somewhat less than in chlorobenzene. This difference may explain the formation of different domain sizes. Despite the difference in the length scale of phase separation, the Debye−Scherrer rings observed in the SAED patterns (insets in the micrographs of Figure 1) indicate that the crystalline structure of PCBM is identical in both films. The broad Debye−Scherrer rings with average *d*-spacings of 0.46, 0.31, and 0.21 nm result from the superposition of many single-crystal diffraction patterns

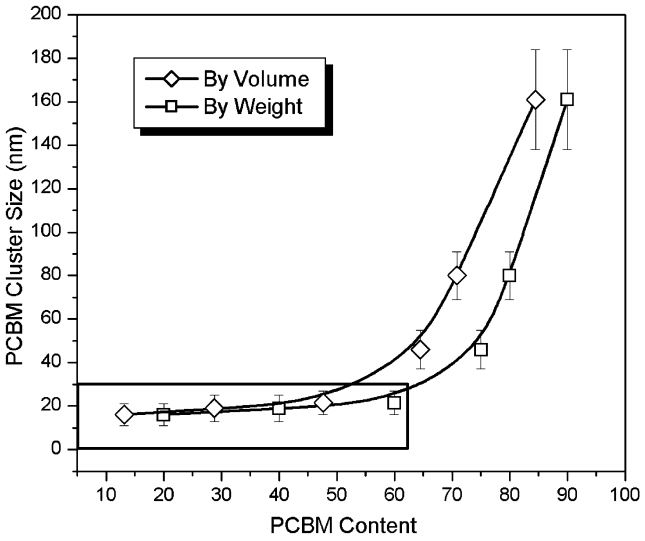

Figure 3. Plot of the average size of PCBM-rich domains in MDMO-PPV:PCBM films spin-coated from chlorobenzene solution vs the PCBM concentration in wt % and in vol %. The specific densities of MDMO-PPV ($\rho = 910$ kg/m^3) and PCBM ($\rho = 1500$ kg/m^3)[33] films were used to convert weight into volume. The solid lines are guides to the eye.

originating from PCBM nanocrystals that are randomly distributed in the PCBM-rich domains. A more detailed discussion of the interpretation of the diffraction patterns of PCBM can be found in ref 28.

The dramatically different morphologies observed in Figures 1 rationalize the strongly different performance of photovoltaic devices fabricated using these solvents.[5,13] The energy conversion efficiency of photovoltaic devices prepared from toluene is approximately $\eta = 0.9\%$, while devices prepared using chlorobenzene give $\eta = 2.5\%$.[5] Apart from possible changes in charge carrier mobility with the change of solvent, the fine phase separation obtained from chlorobenzene provides a larger interfacial area for excitons to dissociate and thereby (at least in part) explains the increased efficiency.

Thin polymer films prepared by spin-coating are usually not in a thermodynamic equilibrium state due to the high rate of solvent evaporation associated with this method. Hence, changing the kinetics of solvent evaporation can influence the film morphology. Drop-casting, for example, reduces the rate of solvent evaporation compared to spin-coating and thereby favors phase separation. Accordingly, the size of the PCBM-rich domains is dramatically increased when the MDMO-PPV:PCBM film is prepared by drop-casting from (the same) chlorobenzene solution rather than by spin-coating (Figure 1c). Drop-casting also results in PCBM-rich domains that are composed of a substantial number of nanocrystals as shown by the SAED (inset in Figure 1c). Therefore, both the nature of the solvent and its evaporation rate are important parameters in determining the morphology of the active layer and thereby the performance of the devices.

Influence of the PCBM Concentration on the Phase Separation. On the basis of the classical theory for describing multicomponent blend (or composite) systems, phase separation should be strongly dependent on the concentration of the components. For this reason, MDMO-PPV:PCBM films were prepared with PCBM concentrations varying from 20 to 90 wt % with respect to the composite film by spin-coating the appropriate

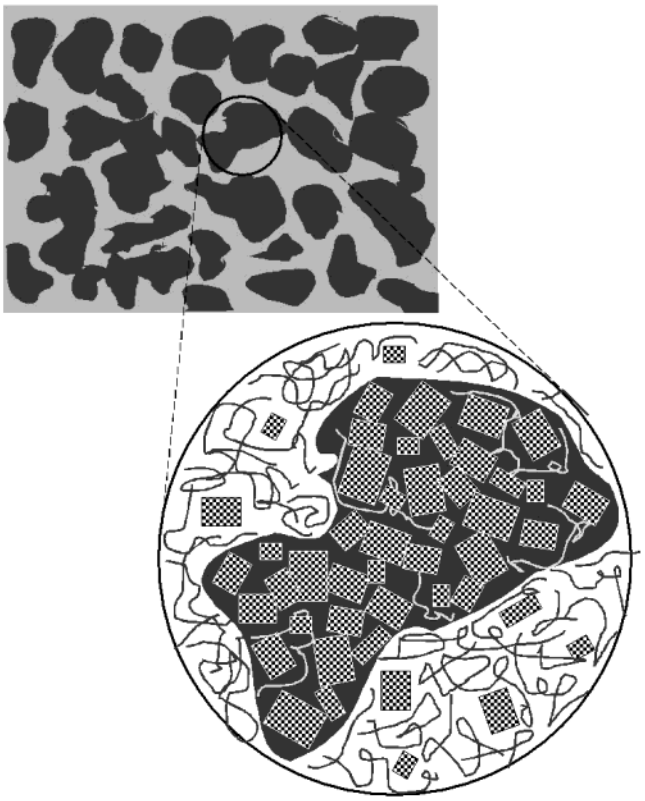

Figure 4. Schematic representation of the MDMO-PPV:PCBM film morphology, in which PCBM-rich domains are composed of PCBM nanocrystals; some PCBM nanocrystals can also be found in the PCBM-poor regions of the films.

mixtures from chlorobenzene solutions. The corresponding bright-field TEM micrographs and SAED patterns are shown in Figure 2. Films with PCBM concentrations up to 60 wt % demonstrate a very homogeneous morphology, and almost no phase separation can be resolved with TEM (Figure 2a−c). However, when the PCBM concentration is increased to around 75 wt %, phase separation between the two components becomes clearly visible, and PCBM-rich domains having a size of about 45 nm can be found (Figure 2d). For higher PCBM concentrations, phase separation becomes more and more pronounced (Figure 2e,f). A plot of the average PCBM cluster size vs its concentration in the blend films is given in Figure 3. It should be pointed out, however, that the data shown in Figure 3 are based on the lateral size of domains inferred from the TEM images. Figure 3 also shows that the development of large PCBM-rich domains starts with PCBM concentration of about 70 wt %.

Within the range of PCBM concentrations investigated, the samples exhibit similar SAED patterns, indicating that the films always contain randomly oriented PCBM nanocrystals. The intensity variations of the SAED patterns inserted in Figure 2 are a result of the different PCBM concentrations used and thus the richness of PCBM crystals. The signal-to-noise ratio of the SAED patterns decreases with decreasing PCBM concentration, but the relative intensities of the three main rings seem to be identical and independent of the PCBM concentration. For the samples with low PCBM concentrations that do not exhibit any resolvable phase separation in the bright-field TEM, we envisage that small nanocrystals are homogeneously dispersed in the polymer matrix. For high PCBM concentrations, these

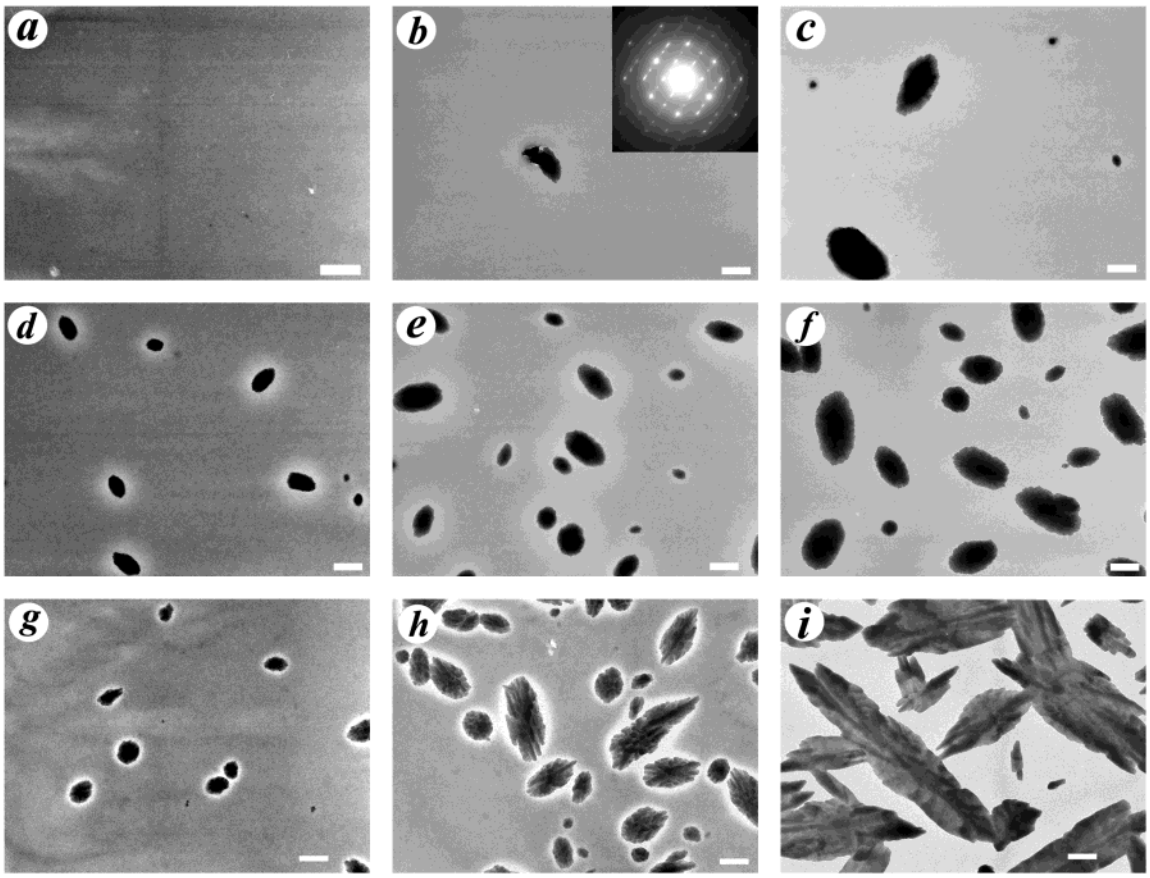

Figure 5. Formation of PCBM single crystals in MDMO-PPV:PCBM thin films upon annealing at 130 °C for PCBM concentrations of 20 wt % (a, b, c), 50 wt % (d, e, f), and 80 wt % (g, h, i). The annealing times are 10 min (a, d, g), 20 min (b, e, h), and 60 min (e, f, i), i.e. increasing from left to right. The dark features in the images are PCBM single crystals (scale bar: 1 μm). The SAED pattern inserted in Figure 5b representatively shows diffraction pattern of the PCBM single crystals obtained.

nanocrystals aggregate into larger almost pure PCBM domains, causing the phase separation observed in Figure 2d−f. Also in these almost pure PCBM domains, many crystallographic orientations are simultaneously present, indicating that nanocrystals are homogeneously distributed in the domains. From these results we conclude that at concentrations above 60 wt % phase separation occurs into a phase that consist of almost pure PCBM and a homogeneous phase that contains MDMO-PPV and PCBM nanocrystals. Figure 4 presents a schematic representation of the MDMO-PPV:PCBM film morphology at high PCBM concentrations.

Thermal Stability of the Morphology of MDMO-PPV:PCBM Films. As shown above, spin-coating provides a simple and successful way to prepare films possessing homogeneous morphology within a relative large area. However, the high rate of solvent evaporation suppresses phase separation, even for a blend that typically would give large-scale phase separation via an equilibrium preparation method. Hence, the spin-coated films are probably not in their equilibrium state, and likely there is a strong thermodynamic driving force for the samples to reorganize toward the stable equilibrium state. This process will be accelerated at elevated temperatures. For solar-cell devices, the morphological reorganization of the active layer with time or temperature may seriously affect the performance and long-term stability.

TEM was used to investigate the changes in phase separation upon annealing of MDMO-PPV:PCBM films at 130 °C for samples with different PCBM concentrations (20, 50, and 80 wt %, Figure 5). Within this concentration range PCBM clusters are formed upon annealing that can be identified in the TEM image as dark areas in a gray MDMO-PPV:PCBM matrix. Notably, the brighter areas initially surrounding the PCBM clusters reflect thinner regions of the film, being composed of almost pure MDMO-PPV (i.e., depleted from PCBM). A detailed discussion related to this feature and the PCBM mobility within the composite film will be the topic of a following study. We note that the dark PCBM clusters visualized in these images are single crystals, as evidenced from the corresponding SAED pattern (inset in Figure 5b).

To investigate the effect of the annealing temperature on the phase separation, we annealed MDMO-PPV:PCBM films with 80 wt % PCBM at temperatures ranging from 60 to 120 °C. Figure 6 shows the corresponding bright-field TEM micrographs and electron diffraction patterns of PCBM single crystals grown under these conditions. Clearly, these PCBM crystals can be classified into two groups by their characteristic appearance. The crystals obtained from the annealing temperatures higher than 80 °C exhibit prominent contrast to their background. However, the crystals obtained from lower annealing temperatures have large sizes in the lateral dimensions but seem to be very thin. Since MDMO-PPV possesses a glass transition temperature (T_g) of around 80 °C, diffusion of PCBM can benefit from the higher conformational dynamics of the polymer chains when the annealing temperatures are above this value. Contrary, for annealing temperatures

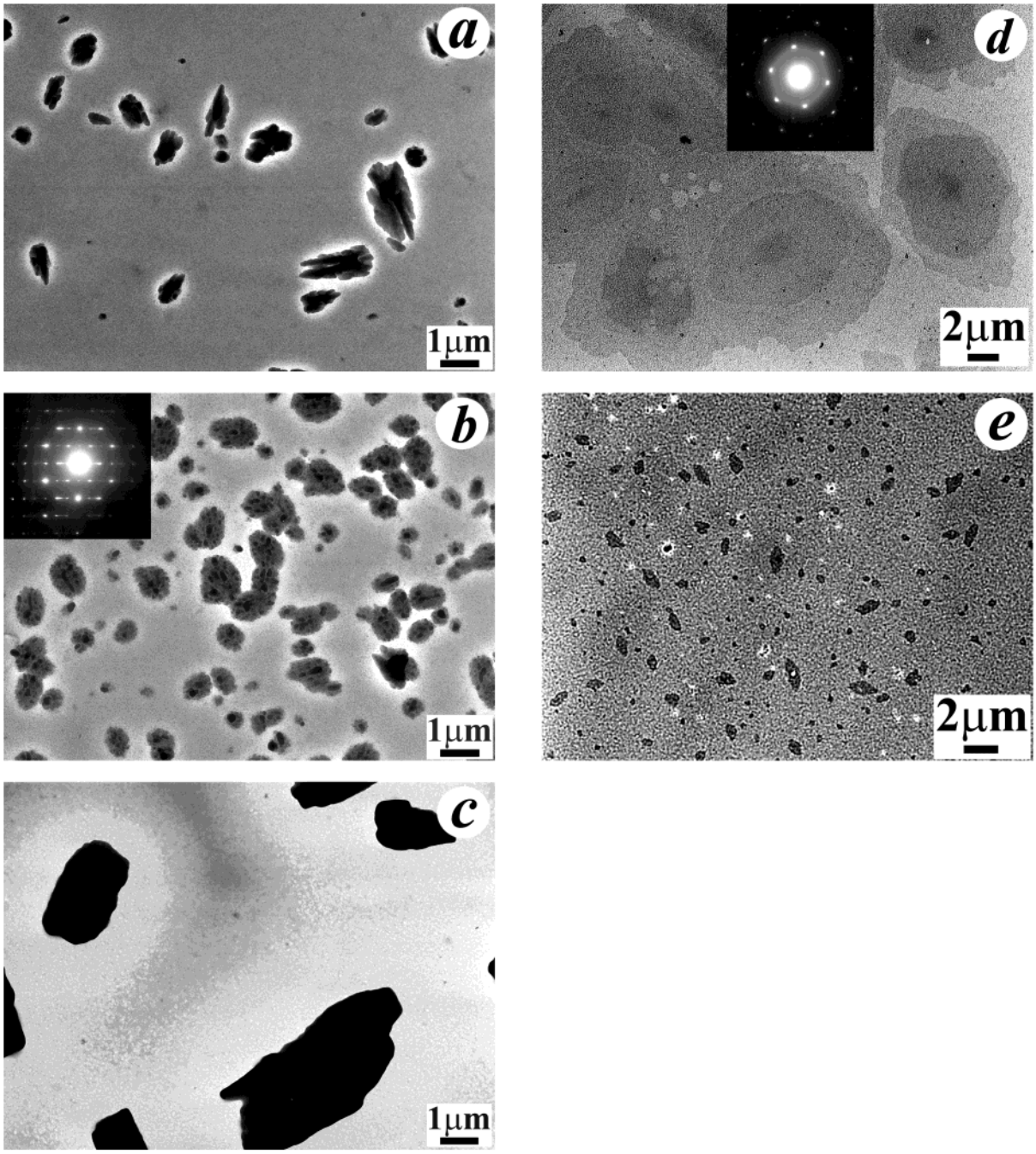

Figure 6. TEM bright-field images of MDMO-PPV:PCBM films (1:4 wt ratio) annealed at temperatures of (a) 120 °C for 50 min, (b) 100 °C for 8 h, (c) 80 °C for 25 h, (d) 70 °C for 80 h, and (e) 60 °C for 120 h. The SAED patterns in Figure 6b,d show typical diffraction patterns of PCBM single crystals.

below the T_g of the polymer matrix, the diffusion mobility of the PCBM molecules is hampered since the polymer matrix is approaching to a chain frozen state. Nevertheless, the diffusion of PCBM does happen at a temperature as low as 60 °C, although the mobility has drastically decreased and annealing times on the order of 1 week have to be applied before changes in the morphology could be detected.

The lifetime of plastic solar cells is one of the problems that must be solved before these devices can compete with traditional photovoltaic technologies. Various mechanisms may cause failure of the active layers in these devices. Both intrinsic processes, such as photochemical reactions or diffusion of species between the various layers during operation, and external factors, such as oxygen or water, may result in chemical change of the active layer,[34,35] the electrode materials, and their interfaces. Some of these processes are accelerated by light and temperature. The results in Figure 6 show that, in addition to these effects, continued phase segregation of the MDMO-PPV:PCBM composite blend with time and temperature may also negatively affect the long-term stability of the active layer.

Conclusion

For bulk heterojunction solar cells, an interpenetrating network structure with nanoscale phase separation is the ideal morphology for high performance. Hence, insights into the parameters that control the morphol-

ogy of the active layer during film formation are required to improve the performance of these devices. In the present study we have demonstrated that both the type of solvent used and its evaporation kinetics have a significant effect on the morphology of MDMO-PPV:PCBM films. Spin-coating from chlorobenzene, which is a good solvent for both components, results in a nanosized phase separation into almost pure PCBM domains that can be visualized with TEM when the PCBM concentration is above 60 wt %. For lower PCBM concentrations, the film morphology appears to be virtually homogeneous from the TEM images. However, all films contain PCBM nanocrystals, independent of the PCBM concentration, as evidenced from SAED. Apparently these nanocrystals are almost homogeneously distributed in the film, while they aggregate and form larger almost pure PCBM domains above the concentration of 60 wt %.

At elevated temperatures, the PCBM molecules can diffuse through the MDMO-PPV matrix and form large single crystals, thereby increasing the dimension and extent of phase segregation. This behavior has been observed for PCBM concentrations as low as 20 wt % in the MDMO-PPV:PCBM films and for annealing temperatures as low as 60 °C, which is ∼20 °C below the T_g of the bulk polymer. Clearly, the limited thermal stability of the morphology of the active MDMO-PPV:PCBM layer will limit the performance and long-term stability of this type of solar cell, even though the kinetics of these processes will likely be reduced when a metal back contact further confines the volume available to the phase separation.[10]

Fortunately, several strategies can be envisaged that may alleviate the limited thermal stability of the morphology. In general, high-T_g polymers will increase the stability of as-prepared morphologies. An elegant example has already been established for the combination of poly(3-hexylthiophene) and fullerene derivatives, where thermal annealing (up to 75 °C) was used to improve the performance.[7,19] Upon cooling to room temperature or normal operating temperatures (possibly up to 75 °C in full sun light), it may be expected that no further changes in the morphology occur as the device has already been annealed at that temperature. Another appealing method to preserve an as-prepared morphology in these blends is by chemical- or radiation-induced cross-linking, analogous to methods recently employed for polymer light-emitting diodes.[36,37] Finally, the use of p−n block copolymers seems an interesting option[38,39] because here phase separation will be dictated by the covalent bonds between the two blocks. Nevertheless, creation of nanoscale bulk heterojunction morphologies that are stable in time and with temperature is one of the challenges that must be met before polymer photovolatics can be applied successfully.

Acknowledgment. The work of X.Y. forms part of the research program of the Dutch Polymer Institute (DPI project #326). J.K.J.v.D. and R.A.J.J. acknowledge financial support from the Dutch Ministries of EZ, O&W, and VROM through the EET program (EETK97115). We thank Prof. J. C. Hummelen and Dr. M. T. Rispens for a generous gift of PCBM and Philips for a generous gift of MDMO-PPV.

References and Notes

(1) Sariciftci, N. S.; Smilowitz, L.; Heeger, A. J.; Wudl, F. *Science* **1992**, *258*, 1474.
(2) Yu, G.; Gao, J.; Hummelen, J. C.; Wudl, F.; Heeger, A. J. *Science* **1995**, *270*, 1789.
(3) Halls, J. J. M.; Walsh, C. A.; Greenham, N. C.; Marseglia, E. A.; Friend, R. H.; Moratti, S. C.; Holmes, A. B. *Nature (London)* **1995**, *376*, 498.
(4) Brabec, C. J.; Sariciftci, N. S.; Hummelen, J. C. *Adv. Funct. Mater.* **2001**, *11*, 15.
(5) Shaheen, S. E.; Brabec, C. J.; Sariciftci, N. S.; Padinger, F.; Fromherz, T.; Hummelen, J. C. *Appl. Phys. Lett.* **2001**, *78*, 841.
(6) Schilinsky, P.; Waldauf, C.; Brabec, C. J. *Appl. Phys. Lett.* **2002**, *81*, 3885.
(7) Padinger, F.; Rittberger, R. S.; Sariciftci, N. S. *Adv. Funct. Mater.* **2003**, *13*, 85.
(8) Svensson, M.; Zhang, F.; Veenstra, S. C.; Verhees, W. J. H.; Hummelen, J. C.; Kroon, J. M.; Inganäs, O.; Andersson, M. R. *Adv. Mater.* **2003**, *15*, 988.
(9) Wienk, M. M.; Kroon, J. M.; Verhees, W. J. H.; Knol, J.; Hummelen, J. C.; van Hal, P. A.; Janssen, R. A. J. *Angew. Chem., Int. Ed.* **2003**, *42*, 3371.
(10) Peumans, P.; Uchida, S.; Forrest, S. R. *Nature (London)* **2003**, *425*, 158.
(11) Bube, R. H. *Photoelectronic Properties of Semiconductors*; Cambridge University Press: Cambridge, 1992.
(12) Pope, M.; Swenberg, C. E. *Electronic Processes in Organic Crystals and Polymers*; Oxford University Press: Oxford, 1999.
(13) Martens, T.; D'Haen, J.; Munters, T.; Beelen, Z.; Goris, L.; Manca, J.; D'Olieslaeger, M.; Vanderzande, D.; De Schepper, L.; Andriessen, R. *Synth. Met.* **2003**, *138*, 243.
(14) van Duren, J. K. J.; Yang, X. N.; Loos, J.; Bulle-Lieuwma, C. W. T.; Sieval, A. B.; Hummelen, J. C.; Janssen, R. A. J. *Adv. Funct. Mater.*, in press.
(15) Halls, J. J. M.; Arias, A. C.; MacKenzie, J. D.; Wu, W. S.; Inbasekaran, M.; Woo, E. P.; Friend, R. H. *Adv. Mater.* **2000**, *12*, 498.
(16) Liu, J.; Shi, Y. J.; Yang, Y. *Adv. Funct. Mater.* **2001**, *11*, 420.
(17) Ditmer, J. J.; Marsegla, E. A.; Friend, R. H. *Adv. Mater.* **2000**, *12*, 1270.
(18) Cabanillas-Gonzalez, J.; Yeates, S.; Bradley, D. D. C. *Synth. Met.* **2003**, *139*, 637.
(19) Camaioni, N.; Ridolfi, G.; Casalbore-Miceli, G.; Possamai, G.; Maggini, M. *Adv. Mater.* **2002**, *14*, 1735.
(20) Yoshino, K.; Hong, Y. X.; Muro, K.; Kiyomatsu, S.; Morita, S.; Zakhidov, A. A.; Noguchi, T.; Ohnishi, T. *Jpn. J. Appl. Phys., Part 2* **1993**, *32*, L357.
(21) Halls, J. J. M.; Pichler, K.; Friend, R. H.; Moratti, S. C.; Holmes, A. B. *Appl. Phys. Lett.* **1996**, *68*, 3120.
(22) Haugeneder, A.; Neges, M.; Kallinger, C.; Spirkl, W.; Lemmer, U.; Feldmann, J. *Phys. Rev. B* **1999**, *59*, 15346.
(23) Kroon, J. M.; Wienk, M. M.; Verhees, W. J. H.; Hummelen, J. C. *Thin Solid Films* **2002**, *403*−*404*, 223.
(24) De Gennes, P. G. *Scaling Concepts in Polymer Physics*; Cornell University Press: Ithaca, NY, 1979.
(25) Forrest, J. A.; Dalnoki-Veress, K.; Dutcher, J. R. *Phys. Rev. E* **1997**, *56*, 5705.
(26) Becker, H.; Spreitzer, H.; Kreuder, W.; Kluge, E.; Schenk, H.; Parker, I.; Cao, Y. *Adv. Mater.* **2000**, *12*, 42.
(27) Hummelen, J. C.; Knight, B. W.; LePeq, F.; Wudl, F.; Yao, J.; Wilkins, C. L. *J. Org. Chem.* **1995**, *60*, 532.
(28) Yang, X. N.; van Duren, J. K. J.; Rispens, M. T.; Hummelen, J. C.; Janssen, R. A. J.; Michels, M. A. J.; Loos, J., accepted in *Adv. Mater.*
(29) Cheng, S. Z. D.; Zhu, L.; Li, C. Y.; Honigfort, P. S.; Keller, A. *Thermochim. Acta* **1999**, *332*, 105.
(30) Yang, X. N.; Kong, X. H.; Tan, S. S.; Li, G.; Ling, W.; Zhou, E. L. *Polym. Int.* **2000**, *49*, 1525.
(31) Yang, X. N.; Tan, S. S.; Li, G.; Zhou, E. L. *Macromolecules* **2001**, *34*, 5936.
(32) Fu, D. S.; Suzuki, H.; Ishikawa, K. *Phys. Rev. B* **2000**, *62*, 3125.
(33) Bulle-Lieuwma, C. W. T.; van Gennip, W. J. H.; van Duren, J. K. J.; Jonkheijm, P.; Janssen, R. A. J.; Niemantsverdriet, J. W. *Appl. Surf. Sci.* **2003**, *203*−*204*, 547.
(34) Sutherland, D. G. J.: Carlisle, J. A.; Elliker, P.; Fox, G.; Hagler, T. W.; Jimenez, I.; Lee, H. W.; Pakbaz, K.; Terminello, L. J.; Williams, S. C.; Himpsel, F. J.; Shuh, D. K.; Tong, W. M.; Jia, J. J.; Callcott, T. A.; Ederer, D. L. *Appl. Phys. Lett.* **1996**, *68*, 2046.

(35) Knol, J.; Hummelen, J. C. *J. Am. Chem. Soc.* **2000**, *122*, 3226.
(36) Müller, C. D.; Falcou, A.; Reckefuss, N.; Rojahn, M.; Wiederhirn, V.; Rudati, P.; Frohne, H.; Nuyken, O.; Becker, H.; Meerholz, K. *Nature (London)* **2003**, *421*, 829.
(37) Hikmet, R. A. M.; Thomassen, R. *Adv. Mater.* **2003**, *15*, 115.
(38) de Boer, B.; Stalmach, U.; van Hutten, P. F.; Melzer, C.; Krasnikov, V. V.; Hadziioannou, G. *Polymer* **2001**, *42*, 9097.
(39) Neuteboom, E. E.; Meskers, S. C. J.; van Hal, P. A.; van Duren, J. K. J.; Meijer, E. W.; Janssen, R. A. J.; Dupin, H.; Pourtois, G.; Cornil, J.; Lazzaroni, R.; Brédas, J.-L.; Beljonne, D. *J. Am. Chem. Soc.* **2003**, *125*, 8625.

MA035620+